

## Conversion of constant-wave near-infrared laser to continuum white light by Yb-doped oxides

Jianhong Wu,<sup>a</sup> Cheng Xu,<sup>b</sup> Jianrong Qiu\*<sup>a</sup> and Xiaofeng Liu\*<sup>b</sup>

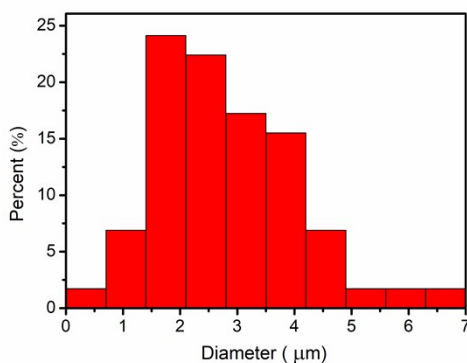
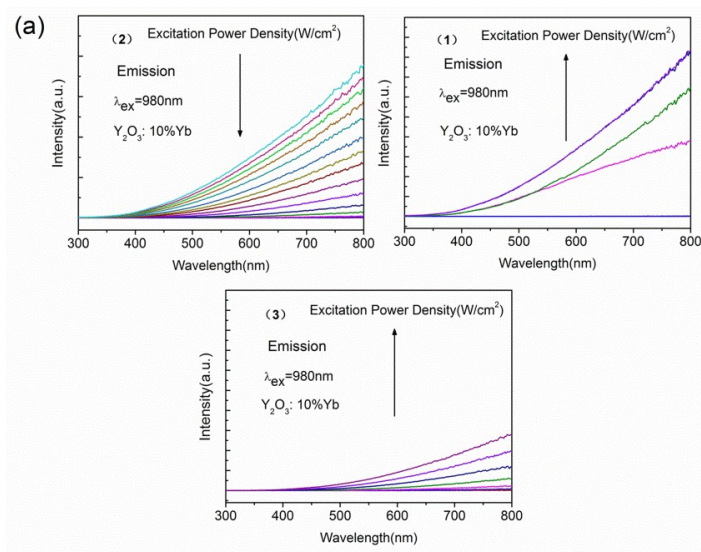


Fig. S1. Grain size distribution determined from the SEM image.

The particles have an irregular shape with a micron-meter scale size and a large size distribution. We calculate the average grain size is about 2.84 μm from the SEM images, as shown in Fig. S1.



<sup>a</sup> State Key Lab of Modern Optical Instrumentation, College of Optical Science and Engineering, Zhejiang University, Hangzhou, 310027, China. E-mail: qjr@zju.edu.cn.

<sup>b</sup> School of Materials Science and Engineering, Zhejiang University, Hangzhou, 310027, China.

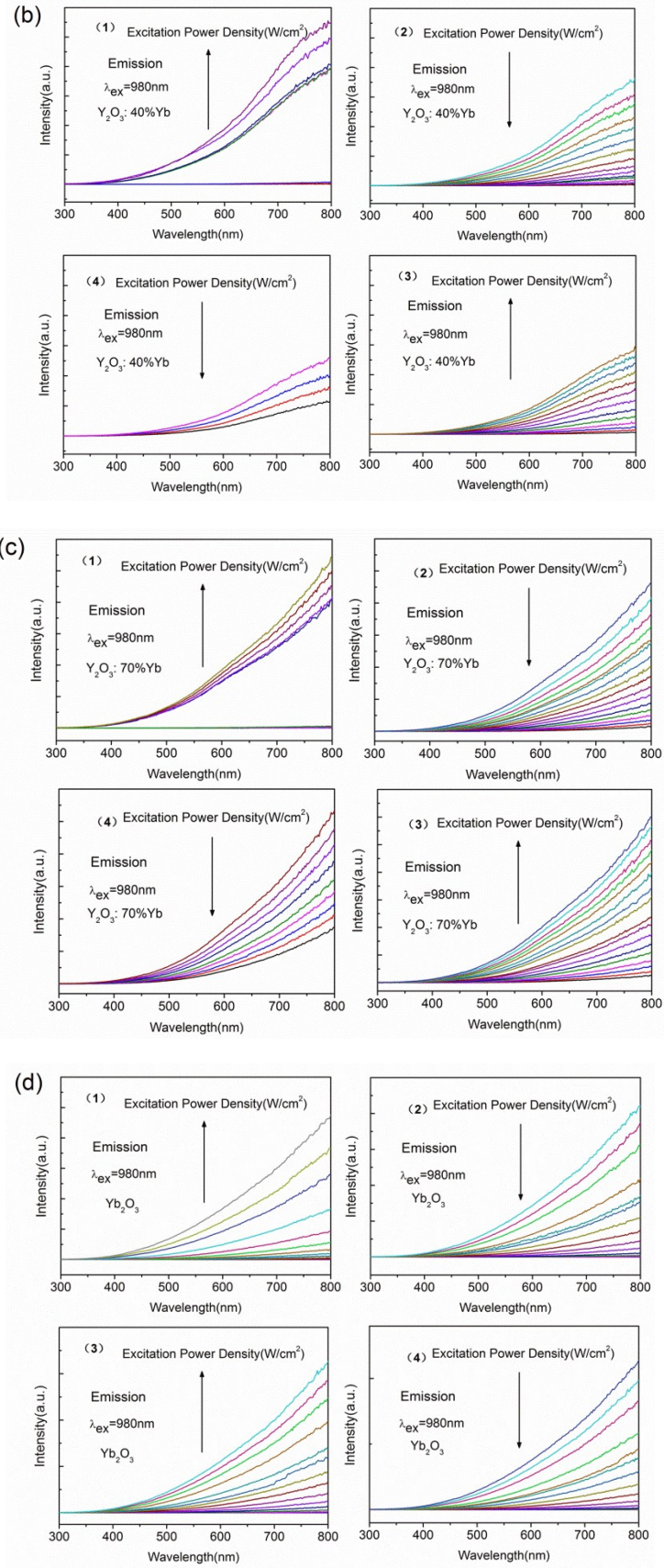


Fig. S2 (a), (b), (c) and (d) Emission spectra recorded by up and down scan of pumping densities for  $Y_2O_3: x\%Yb^{3+}$ ,  $x=0, 10, 40, 70, 100$ , respectively. (1) and (3) are up-scans and (2) and (4) are down-scans respectively.

The power dependence of the white light emission spectra in  $Y_2O_3$ :  $x\%Yb^{3+}$ ,  $x=0, 10, 40, 70, 100$ ) microcrystals are shown in the Fig. S2. The growth of white light emission intensity is dependent on excitation laser power density. All the white light emission intensity shows a clear threshold pump density ( $P_{th}$ ), characterized by an up-jump in emission intensity at the threshold (Fig. 4). And heat accumulation is need only in the first up-scan to trigger the transition from stage II to stage III (given in the Fig. 3) to produce white light, while the slow cooling of the samples makes the accumulation of heat completely unnecessary in the following up and down-scans.

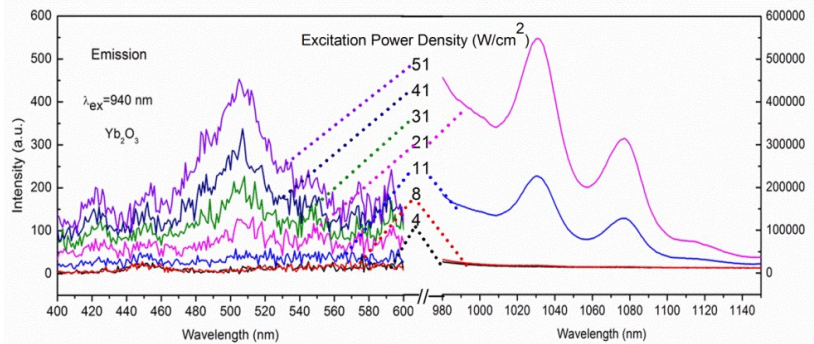


Fig. S3 The spectra of the cooperative luminescence of  $Yb^{3+}$  around 500 nm and the luminescence of  $Yb^{3+}$  (by the transition of  ${}^2F_{5/2} \rightarrow {}^2F_{7/2}$ ) in the NIR range recorded at low pumping densities.

The growth of visible and infrared emission intensity is dependent on excitation laser power density. As shown in Fig. S3, the overall white light emission intensity is found to increase with the increasing power density. Significantly, when the excitation power density reaches 11  $W/cm^2$ , infrared emission is observed, but no visible light. The visible light emission occurs at 21  $W/cm^2$ . This is to say, the threshold of blue-green emission is significantly higher than that of infrared. It also further illustrate that the 500 nm blue-green emission is formed by  $Yb^{3+}$ - $Yb^{3+}$  pairs.

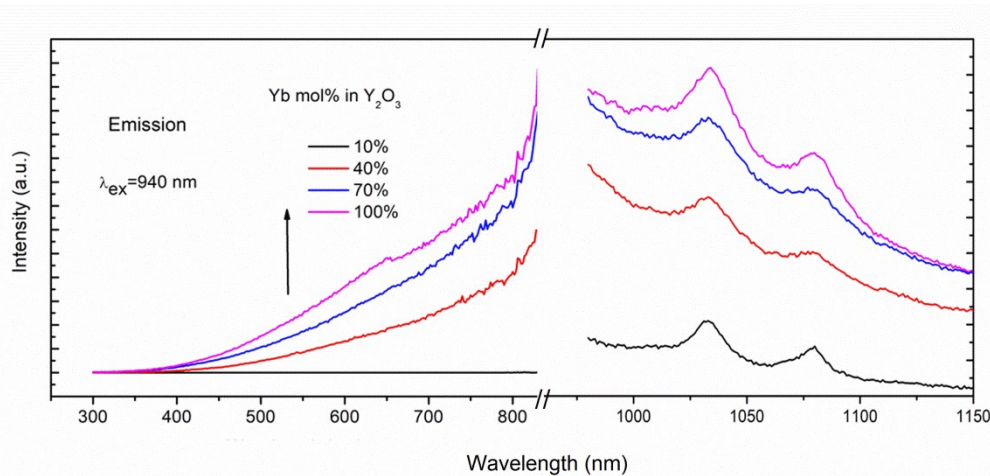


Fig. S4 Spectra of  $Y_2O_3$ :  $x\%Yb^{3+}$  ( $x=0, 10, 40, 70, 100$ ) upon the same pumping densities of 320  $w/cm^2$ .

PL spectra of  $Y_2O_3$  doped with different  $Yb^{3+}$  concentrations upon the same condition are shown in Fig. S4. The white light emission threshold decreases monotonically with the increasing  $Yb^{3+}$  concentrations. It illustrates that the white light emission relates to  $Yb^{3+}$  ions, and the  $Yb^{3+}$  acts as a heat accumulation ions which has a large absorption for the NIR laser, resulting in a much smaller  $P_{th}$  eventually.

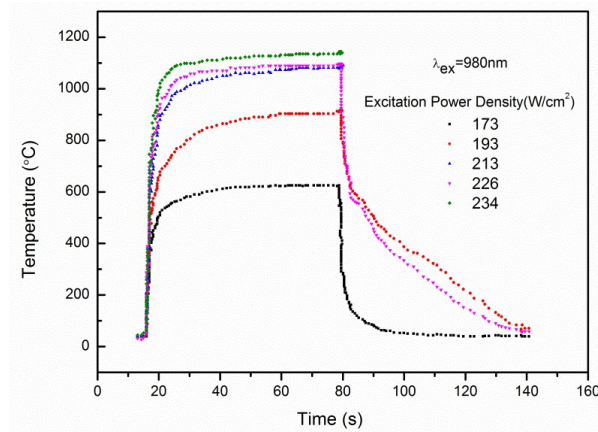


Fig. S5 Temperature rise of  $\text{Yb}_2\text{O}_3$  microcrystals probed by a thermal camera with different pump power density.

The infrared thermal camera, which can automatically capture the spot with the highest temperature, is used in our experiment. As shown in Fig. S5, the temperature increases with increasing excitation power density. The emission intensity (shown in Fig. S2) shows the same change trend. This result further evidence that this phenomenon is relate to temperature.

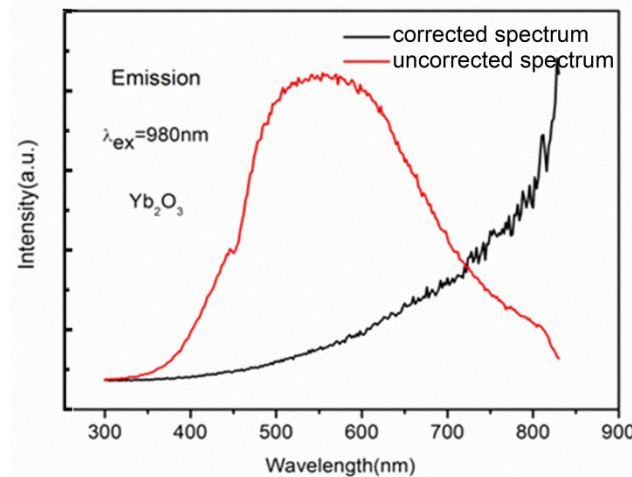


Fig. S6. The spectra of  $\text{Yb}_2\text{O}_3$  microcrystals before (red) and after (black) correction for detector efficiency.

In the literature, there are two main kinds of mechanism for this phenomenon.<sup>1-4</sup> The first mechanism is the laser-driven blackbody radiation. However, the sample temperature is too low to confirm this theory. And according to Wien's displacement law the peak of the blackbody radiation ( $\lambda_p$ ) and the sample temperature ( $T$ ) follows this relation:  $\lambda_p \propto T^{-1}$ , which is not found in the present experiment. On the other hand, these calculated spectra (shown in Fig. 7a) are strongly red shifted compared with the observed spectra in this work and also other reports.<sup>2, 5</sup> The second mechanism is based on charge transfer emission of  $\text{Yb}^{3+}$  ion associated with the transient interconversion of  $\text{Yb}^{3+}$  to  $\text{Yb}^{2+}$ , or  $\text{Eu}^{3+}$  to  $\text{Eu}^{2+}$ , which feature an broad emission "peak" at 500 -800 nm. But as shown in Fig. S6, the emission spectra corrected or uncorrected are different. After the spectral calibration, the "peak" disappears and the maximum intensity is in the spectral range between 900 -1000 nm.<sup>5</sup>

## References

- 1 L. Li, H. Li, Z. Zhang, X. Zhang, J. Zhao and J. Cui, *Appl Phys B*, 2014, **116**, 867.
- 2 H. Ye, V. Bogdanov, S. Liu, S. Vajandar, T. Osipowicz, I. Hernández and Q. Xiong, *The J Phys Chem Lett*, 2017, **8**, 5695..
- 3 M. Stefanski, M. Lukaszewicz, D. Hreniak and W. Strek, *J Chem Phys*, 2017, **146**, 104705.
- 4 W. Strek, R. Tomala, M. Lukaszewicz, B. Cichy, Y. Gerasymchuk, P. Gluchowski, L. Marciniak, A. Bednarkiewicz and D. Hreniak, *Scientific reports*, 2017, **7**, 41281.
- 5 G. Bilir, G. Ozen, J. Collins, M. Cesaria, B. Di Bartolo, *IEEE Photonics J*, 2014, **6**, 1.